

Evaluation of Mechanical and Thermophysical Properties of Chitosan/Poly(DL-Lactide-co-Glycolide)/Multiwalled Carbon Nanotubes for Tissue Engineering

Imelda Olivas-Armendáriz¹, Elí Santos-Rodríguez², Susana Correa-Espinoza³,
Dorian-Said Domínguez-Domínguez³, Illian Márquez-Méndez¹, Mónica Mendoza-Duarte⁴,
María-Concepción Chavarría-Gaytán¹, Santos-Adriana Martel-Estrada^{5,*}

¹Instituto de Ingeniería y Tecnología, Universidad Autónoma de Ciudad Juárez, Chih., México

²Mesoamerican Centre for Theoretical Physics, UNACH, Ciudad Universitaria Carretera Emiliano Zapata Km. 4, Chiapas, México

³Instituto de Ciencias Biomédicas, Universidad Autónoma de Ciudad Juárez, Chih., México

⁴Centro de Investigación en Materiales Avanzados, Departamento de Integridad y Desarrollo de Materiales Compuestos, Chihuahua, México

⁵Instituto de Arquitectura, Diseño y Arte, Universidad Autónoma de Ciudad Juárez, Chih., México

Abstract Chitosan (Ch), Poly(DL-lactide-co-glycolide) (DL PLG) and Multiwalled Carbon Nanotubes (MWCNT) were used to fabricate biodegradable porous scaffolds for applications in tissue engineering by thermally induced phase separation (TIPS) technique. Through the use of a Field Emission Scanning Electron Microscopy, the variation in porous morphology was studied. The cumulative results obtained from IR and X-ray diffraction spectra, TGA, DSC and Mechanical properties suggest that there is a chemical interaction between the components of the composite. Also, *In vitro* cell culture of Wistar rat's osteoblasts were used to evaluate the phenotype expression of cells in the scaffolds, characterizing the viability and alkaline phosphatase (ALP) activity. Moreover, it was confirmed the mineralization of the cells by IR spectra and EDS analysis. Our results thus show that Ch/DL PLG/MWCNT scaffolds are suitable for biological applications.

Keywords Chitosan, Poly DL lactide-co-glycolide, MWCNT, Thermal properties, Mechanical properties, Biocompatibility

1. Introduction

Bone tissue has limited ability to self-repair defects due to trauma or diseases that may not heal and result in non-union problems. This situation must be aided by the use of bone substitutes or bone grafts [1]. Tissue engineering is a disciplinary field focused on the development of solutions of critical problems related with tissue loss and organ failure. The substitutes developed must be able to restore, maintain or improve tissue function. For these reasons, the materials used for tissue engineering must stimulate specific cell response at molecular level to favour cellular attachment, proliferation, differentiation and extracellular matrix production. Also, the biomaterial must have adequate mechanical properties and biocompatible surface [2], nontoxic, being biodegradable and adequate for the diffusion of gases and nutrients [3].

Biocompatible natural and synthetic materials including polymers and ceramics have been studied for their potential use for the repair and regeneration of bone defects [1]. The biodegradable polymers that are used for this purpose includes polylactic acid (PLA), polyglycolic acid (PGA), polyanhydrides, polyfumarates (PF), polyorthoesters and polycaprolactones [4]. Previously, a Chitosan/PLGA composite has been tested for bone engineering, showing evidence of enhanced alkaline phosphatase activity and elevated gene expression of osteoblast-specific markers [1]. Also, derivatives of PLGA such as poly(D,L-lactide-co-glycolide) have been used in a composites with hydroxyapatite for drug release and to promote osteointegration [5]. The poly(lactide-co-glycolide) (PLGA) is a biodegradable polymer that does not require surgical removal and can be processed in different shapes. Also, it is a biodegradable polymer with good biocompatibility [6].

On the other hand, chitosan is a heteropolysaccharide consisting of poly $\beta(1,4)$ -D-glucosamine units, and it is cationic polysaccharide obtained by the alkaline deacetylation of chitin, the main component of exoskeletons of crustaceans and insects [7, 8]. Chitosan has been used in

* Corresponding author:

mizul@yahoo.com (Santos-Adriana Martel-Estrada)

Published online at <http://journal.sapub.org/materials>

Copyright © 2015 Scientific & Academic Publishing. All Rights Reserved

diverse tissue engineering applications due to its low cost, antimicrobial activity and biocompatibility [9].

Carbon nanotube combined with different materials has received enormous interest because of their potential applications in medicine and solar cell field [10]. It has been used as a filler in polymer based composites, in order to improve mechanical, electrical and thermal properties of composites [11, 12]. Carbon nanotubes have an excellent potential to improve those characteristics due to their small dimensions, high aspect ratio (length to diameter), strength and stiffness [13].

Previously, our group dedicates efforts to produce a homogenous mixture of poly (DL, lactide) and chitosan by phase separation method [14] in which it was investigated the behavior of primary osteoblast cultured in the scaffold [15]. The composite developed showed good proliferation maintaining the osteogenic phenotype, but the mechanical and thermo-physical properties had to be yet improved. Carbon nanotubes have shown the potential to improve the mechanical properties of a polymer-based composites, but bioactivity and biocompatibility must be tested.

In order to evaluate the potential applications in bone engineering, a chitosan/poly (DL-lactide-co-glycolide / Multiwalled carbon nanotubes) (Ch/DL PLG/MWCNT) composite was produced as a scaffold using thermally induced phase separation. Therefore, in this work, the synthesis, morphology, FTIR, X-ray diffraction spectra, mechanical and thermal characterization of these composites is describe. Moreover, in this study we investigated the behavior of primary osteoblast cultured in the presence of chitosan and poly(DL-lactide-co-glycolide)/MCWNT composite scaffold. Then, biomineralization, alkaline phosphatase (ALP) activity, cell viability and DNA quantification of osteoblasts in the scaffolds were evaluated.

2. Materials and Methods

2.1. Materials

Chitosan (310,000-375000 Da and 75-85% deacetylated) was purchased from Sigma-Aldrich (United States). 75:25 Poly (DL-lactide-co-glycolide) with an inherent viscosity range of 0.55-0.75dK/g in CHCl_3 was purchased from Lactel (United States). Glacial Acetic Acid (Mallinckrodt, United States) was used as solvent.

Chitosan/Poly (DL-lactide-co-glycolide)/Multiwalled carbon nanotubes was prepared using the thermally induced phase separation technique. The MWCNT were fabricated and purified in our laboratory by spray pyrolysis method according with a previous published work [16]. Chitosan/DL PLG composites at 70/30 composition were prepared to add MWCNT with different concentrations. The composites were prepared by a previous reported procedure [14]. Firstly, measured percentage of the purified MWCNT was dispersed in 1% (v/v) aqueous glacial acetic acid by sonication for 5 minutes at room temperature. Then, Chitosan was added to

the MWCNT solution and mixed together. Following, 5% (% w/v) DL-PLG in chloroform was added to the Chitosan / MWCNT solution at a rate of 1 drop/minutes, approximately. After the DL PLG solution was completely added to the chitosan solution, the solution was stirred for one hour followed by 10 minutes of sonication in order to eliminate the gas from the mixture. After this process, each composite was frozen at -78°C for 6 hours. The solvent was then extracted by a freeze drying system Labconco FreeZone 2.5. The composites were neutralized at -20°C by immersion in ethanol during 12 hours followed by another 12 h immersion into $\text{NaOH-CH}_3\text{CH}_2\text{OH}$ aqueous solution (prepared using an 80 % ethanol aqueous solution mixed previously with 0.5(w%/w%) of NaOH). Then the samples were washed and rinsed with distilled water.

2.2. Physical Characterization of the Samples

In order to make the chemical characterization of the composites FTIR-ATR spectrometer Nicolet 6700 was used. Each dried sample was used without any special preparation for the FTIR scan. All spectra were recorded using 100 scans and 32 cm^{-1} resolution. Also, all FTIR spectra were recorded as absorbance values at each data point in triplicate. The X-ray diffraction patterns of the samples were analyzed at 2θ values between 5° and 80° with a step size of $2\theta=0.02^\circ$ in an X-ray diffraction instrument in continuous mode (PANanalytical X'Pert PRO). The morphology was analyzed in a Field Emission Scanning Electron Microscope JEOL JSM-7000F. The average pore size and the pore size distribution were measured using the Scandium Universal SEM Imaging Platform software (Soft Imaging System) from the SEM micrographs in the original magnification. Three different cross-section of each scaffold were used to estimate the pore size and at least 100 pores to estimate the distribution.

Thermogravimetric analysis (TGA) of Chitosan/DL PLG/MWCNT composites was carried out using TG analyser (SDT Q600 from TA Instruments, United States). The dry samples were heated from room temperature to 750°C at $10^\circ\text{C}/\text{minutes}$ under nitrogen atmosphere with a flow rate of 80 mL/minutes. The first derivative of the mass-change with respect to time (DTG) was calculated and plotted as a function of the temperature. Differential Scanning Calorimetric (DSC) measurements were carried out on DSC Q200 V200 V24.8 Build 120 (TA Instruments, United States). The samples were cooled from room temperature to -50°C at a rate of $20^\circ\text{C}/\text{minutes}$. Finally, they were heated from -50°C to 250°C at $10^\circ\text{C}/\text{minutes}$ under an argon atmosphere at 80 mL/minutes. The reproducibility of TGA/DSC analysis was checked by analyzing three samples from each scaffold. From the weight decrease between 200°C and 400°C , the relative error was 3.1 %. In the case of remaining weight at 750°C , the relative error was 2.88%. RSA III (Rheometrics Analyzes System) TA was used in static mode at a frequency of 6.2832 rad/s and 37°C . Disks of approximately 10 mm in thickness and 25 mm in diameter

were used in all the experiments. Three samples of each composition were measured and mounted in a compression clamp.

2.3. Biological Characterization of the Samples

Rats Sprague Dawley (14-days old) were used for the isolation of osteoblasts from calvarian. The isolation was made using a previously published method [15]. Briefly, the calvaria tissue were dissected and prepared by enzymatic digestion using collagenase (type I) in phosphate buffered saline (PBS) at 37°C. The cells were dissociated by repeated pipetting. National guidelines for the care and use of laboratory animals were observed.

For the culture, it was used 3 scaffolds of each sample (1 cm²) for the different biological tests previously sterilized in an ethanol bath for 5 minutes and washed with sterile DI water. The scaffolds were placed in a 24 well-culture plate and exposed to UV light for 2 hours. After the UV sterilization, 300 µl of α -Mem supplemented with 10% fetal bovine was added to each scaffold and incubated at 37°C overnight for degasification.

After this procedure, 50,000 osteoblasts calvaria cells were pooled into the scaffolds and cultured in the prepared solution of α -MEM supplemented with 10% fetal bovine, 1% antibiotics, 2.1 mg/ml β -glycerophosphate and 50 µg/ml ascorbic acid in an incubator at 37°C with 5% CO₂. The medium was replaced carefully every 2 days without disturbing the samples. Cultures were finished at 1, 3 and 7 days.

After the incubation period, the samples were rinsed with PBS (pH 7.4), and immersed in PBS containing 3% Glutaraldehyde for 4 h to fix the cells, followed by rinsing with PBS for 10 minutes. They were dehydrated with ethanol solutions (from 30% to 100%) for additional 30 minutes, being allowed to dry. A Field emission scanning electron microscopy JEOL JSM-7000F coupled with an energy-dispersive system EDS 7557 INCA Oxford Instruments (England) was used to characterize the morphology and to observe cell proliferation on the surface of the sample.

The alkaline phosphatase (ALP) activity of the osteoblasts on the scaffolds was measured. A set of control and test cultures were harvested on days 1, 3 and 7 and washed twice with PBS. The osteoblasts were lysed with 1% Triton X-100 in DEPC-treated water and three freeze-thaw cycles at -70°C. The alkaline phosphatase activity in the lysed cells was determined using an alkaline phosphatase substrate assay kit (Pierce biotechnology, Monterrey, Mexico) with p-nitrophenyl phosphate as substrate. The alkaline phosphatase activity was measured at 405 nm (Microplate spectrophotometer Bench mark plus, BIO-RAD).

The MTT assay was performed for viability analysis of the cells. After incubation, the well plates were taken out from the incubator, eliminated all the media, plates were washed with PBS and 50 µL of MTT solution (5mg/mL in PBS) was added in each well. After incubation for 3 h, 400 µL of

DMSO (dimethyl sulfoxide) was added in each well and it was leave in repose for 30 minutes. 100 µL of this solution was shifted to the 96-well plate. The optical density was measured using microplate reader (Bench mark plus, BIO-RAD) at 570 nm. Positive controls were also prepared for comparison purpose. Furthermore, Pico Green Assay (Invitrogen) was used to measure the DNA content of the samples incubated with osteoblast for proliferation, following the manufacturer's protocol.

Finally, the data obtained were evaluated for statistical significance using the Student's t-test. The results are reported as mean \pm SD and the differences observed between composites results were considered significant when $p < 0.05$.

3. Results

3.1. Morphology

In Figure 1 the morphology of the composites is shown where a porous structure can be appreciated, the lyophilized and neutralized composites present a porous structure with the MWCNT embedded into a continuous polymeric matrix. A higher magnification shows that inside the big porous of the composites exist a highly interconnected porous structure (<20 µm porous) (Table 1). Figure 2 shows the changes in the polymeric matrix as the MWCNT content increases inside it. These changes show that as the MWCNT content increases the porosity is less interconnected than in the chitosan composite, possible due to an increase of internal stress in the matrix produced by the nanotubes.

Table 1. Pore size distribution of the Ch/DLPLG/MWCNT composites. Three different cross-section of each scaffold were used to estimate the pore size and at least 100 pores to estimate the distribution

Composite Ch/DLPLG / MWCNT	Porosity %	<50 (µm) %	50-150 (µm) %	150-250 (µm) %
70/30/0%	67.07 \pm 3.02	36.36	57.39	6.25
70/30/10%	84.58 \pm 2.10	41.42	51.51	7.07
70/30/15%	69.49 \pm 4.51	50.86	44.00	5.14
70/30/20%	78.72 \pm 3.23	32.32	57.58	10.10

4. Results

4.1. Morphology

In Figure 1, the morphology of the composites is shown where a porous structure can be appreciated. The lyophilized and neutralized composites present a porous structure with the MWCNT embedded into a continuous polymeric matrix. A higher magnification shows that inside the big porous of the composites exist a highly interconnected porous structure (<20 µm porous) (Table 1). Figure 2 shows the changes in the polymeric matrix as the MWCNT content increases inside it. These changes show that as the MWCNT content increases the porosity is less interconnected than in the

chitosan composite, possible due to an increase of internal stress in the matrix produced by the nanotubes.

4.2. FTIR Analysis of the Composites

Infrared spectroscopy (FTIR) is an analytical technique that measures the absorption of various infrared light wavelengths by the material identifying specific molecular components and structures [11]. Figure 3, shows that the N-H bending vibration of chitosan band shifted from 1556.3 cm^{-1} to 1554.4 cm^{-1} , 1555.3 cm^{-1} and 1544.5 cm^{-1} , respectively for 10%, 15% and 20% composites. The spectra of 20% composite show a reduced intensity on the band at 1069.7 cm^{-1} , that could imply an interaction of the ether bond of chitosan with the poly(lactide-co-glycolide) and the MWCNT. The spectra of composites show a band between 1409 cm^{-1} and 1426 cm^{-1} assigned to the CH_3 bonds of DLPLG. This spectra show a pronounced band at 1741 cm^{-1} that corresponds to C=O bond of the DLPLG that increases its intensity as the content of MWCNT increased in the composites. The FTIR spectra of composites show also the main absorption peaks of carbon nanotubes. Band corresponding to O-H deformation and C-O stretching [17] was shifted from 1220 cm^{-1} to 1217.6 cm^{-1} and 1219.3 cm^{-1} , respectively for 15% and 20% composites and increase as the content of MWCNT increase in the composite. The band was not evident in the 10% composite. Thus, it could be possible the existence of hydrogen bonds between the amino groups of chitosan and carboxyl groups of DL PLG or hydroxyl groups of chitosan and carboxyl groups of DL PLG as it was suggested by previous research [14, 15].

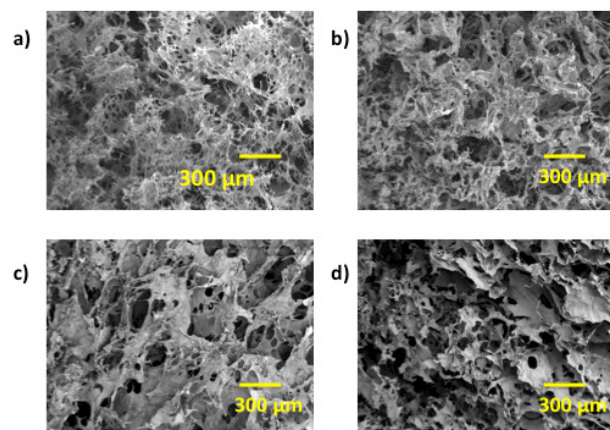


Figure 1. SEM Micrographs of Ch/DLPLG/MWCNT composites: a) 70/30/0 Ch/DLPLG/MWCNT, b) 70/30/10% Ch/DLPLG/MWCNT, c) 70/30/15% Ch/DLPLG/MWCNT and d) 70/30/20% Ch/DLPLG/MWCNT

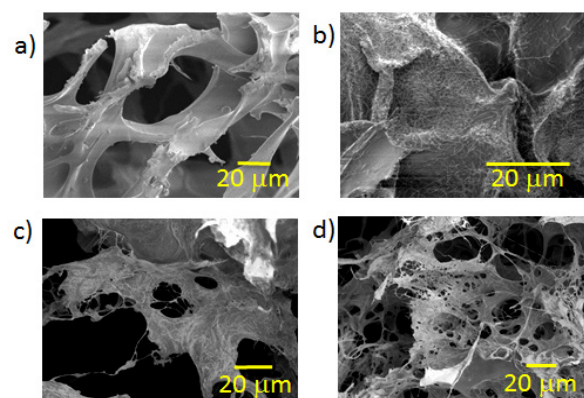


Figure 2. SEM Micrographs of Ch/DLPLG/MWCNT composites: a) 70/30/0 Ch/DLPLG/MWCNT, b) 70/30/10% Ch/DLPLG/MWCNT, c) 70/30/15% Ch/DLPLG/MWCNT and d) 70/30/20% Ch/DLPLG/MWCNT

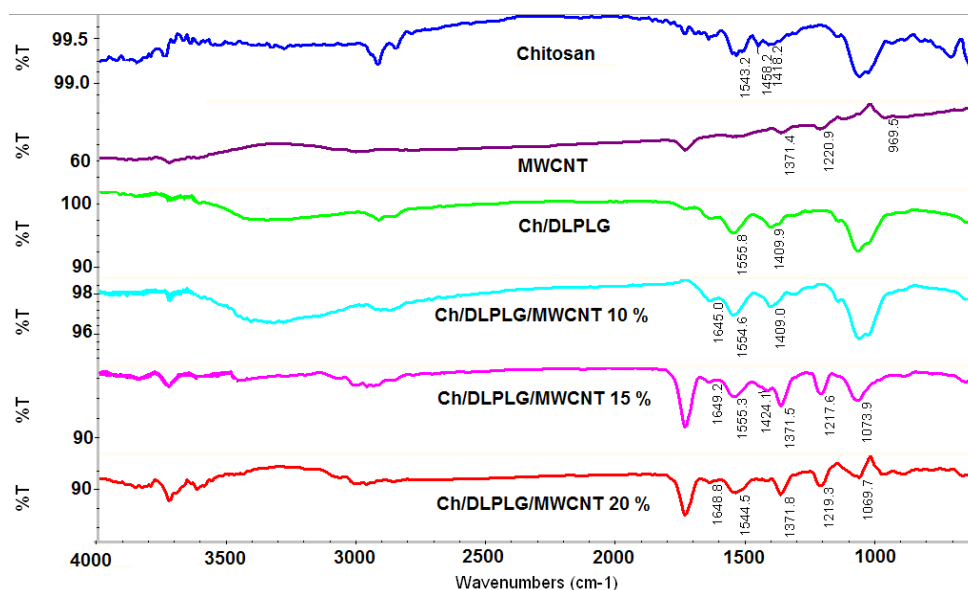


Figure 3. FTIR spectra of the Ch/DLPLG/MWCNT scaffolds. All FTIR spectra were recorded as absorbance values at each data point in triplicate

4.3. Thermal Analysis of the Composites

The TGA thermograms for 70/30/0 Ch/DLPG/MWCNT composite and samples with MWCNT content, 70/30/10%, 70/30/15% and 70/30/20% are shown in Figure 3a. It was observed that the thermal stability of the original composite (70/30/0 Ch/DLPG/MWCNT) improved by addition of MWCNT. In general, the TGA profiles of the Ch/DLPG / MWCNT composites showed that it will decompose before melting. The Ch/DLPLG composite was thermally decomposed in the region of 228°C and 391°C as shown in Figure 4. This thermal decomposition could be attributed to the dehydration of the saccharide rings and followed decomposition of chitosan backbone [18] and the main decomposition of the DLPLG [14].

In general, as the percentage of MWCNT increases, the thermal stability of the composites increases as well, with the percentage of decomposition improved from 97.27% to 88.24% for the Ch/DLPLG and Ch/DLPLG/20% composite, respectively. The initial temperatures of maximum decomposition were diminished from 306.06° to 285.56°C for the original and the 20% MWCNT content composite, respectively.

There are two main stages of degradation in the TGA curve of all samples. The initial weight loss of the composites (100-150°C) is due to evaporation of the water.

This loss depends on the initial moisture content of the composites as it was previously reported [14]. The severe weight loss is called main region of decomposition in Table 2. It is due to the decomposition of the major components of the composites. The weight-loss percentage of all samples was differentiated and the derived data are depicted in Table 2. The DTG profiles show that the Ch-DL PLG and MWCNT composites have only single peak for all composites, indicating that the chemical interaction between Chitosan-DLPLG and MWCNT resulted in a relatively homogenous composition of the blends as is shown in the Figure 3b. The T_{max} corresponds to the temperature at the maximum degradation rate. All MWCNT-composites exhibit a single peak of fast thermal degradation. As it is showed in Table 2 an improved thermal stability was achieved for the composites as MWCNT content increased due to the chemical interactions between the substances. Chitosan is a semi-crystalline polymer with strong inter- and intra-molecular hydrogen bonds [14]. The T_g determined was 348.70 °C, 329.92 °C, 347.05 °C and 323.25 °C for Ch/DL PLG, Ch/DLPLG/10%, Ch/DLPLG/15% and Ch/DLPLG/20% respectively. As it can be seen, the T_g moved to a lower value as the percentage of MWCNT is increased. These results are only evidence of a partial miscibility

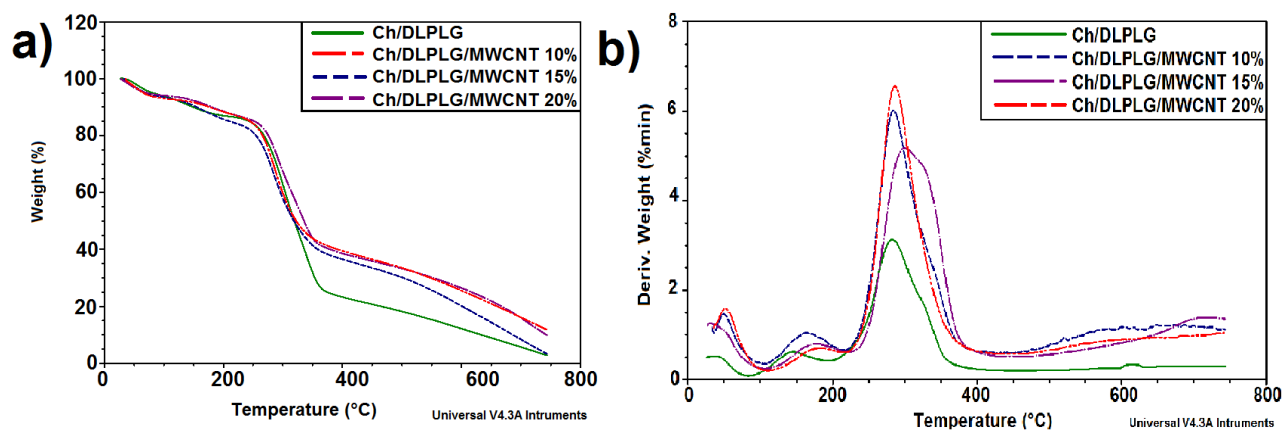


Figure 4. a) Thermal decomposition and b) DTG profiles of chitosan/DLPLG/MWCNT composites. The reproducibility of TGA/DSC analysis was checked by analyzing three samples of each scaffold

Table 2. Thermal degradation of the composites

Composite Ch/DLPLG/ MWCNT	Main region of decomposition (°C)	Weight percentage of decomposition %	T_{max} (°C)	Maximum degradation velocity (%/ minutes)
70/30/0%	228-391	97.27	306	6.540
70/30/10%	247-354	96.70	284	6.018
70/30/15%	249-382	90.10	293	5.610
70/30/20%	246-355	88.24	285	6.675

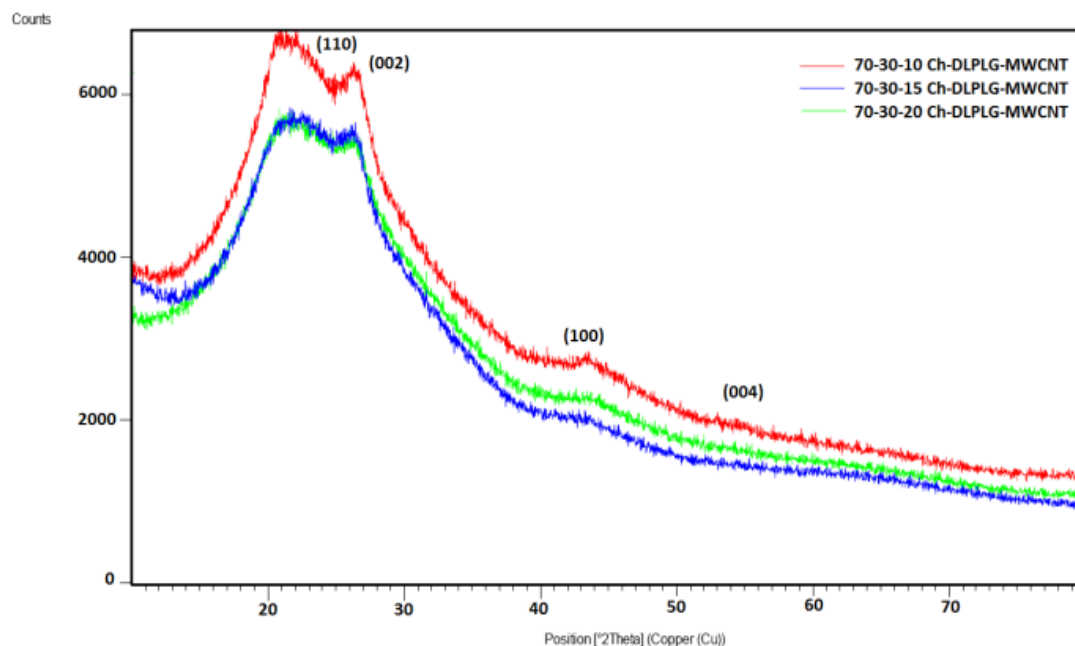


Figure 5. X-ray diffraction spectra of composites. The diffraction peaks in all the plots are in agreement with chitosan and MWCNT XRD peaks reported by literature [20, 21]

Table 3. Mechanical properties of the composites. Three samples of each composition were measured and mounted in a compression clamp

Composite Ch/DLPLG/ MWCNT	Elastic Module (E) (Pa)	Compression strength (Pa)	Deformation at the maximum strength (%)	σ_{10} (Pa)
70/30/10%	$132,411 \pm 3985$	$0.19 \times 10^5 \pm 500$	29.20 ± 0.07	$0.14 \times 10^4 \pm 65$
70/30/15%	$206,047 \pm 6062$	$0.41 \times 10^5 \pm 834$	24.06 ± 0.36	$1.14 \times 10^4 \pm 834$
70/30/20%	$208,259 \pm 1357$	$0.45 \times 10^5 \pm 612$	23.37 ± 0.24	$2.35 \times 10^4 \pm 36$

4.4. X-ray Diffraction Results

Figure 4 shows XRD pattern of Ch-DLPLG and the MWCNT composites. The pure chitosan sample is amorphous with a halo that peaks around $2\theta=21.70^\circ$. This peak is in agreement with other published results [14, 19]. This reflection corresponds to the regular crystal lattice (110) of chitosan [20]. The graphite peak of plane 002 at $2\theta=25.8^\circ$ is clear in patterns. The other diffraction peaks related with MWCNT at the angle $2\theta = 42.7^\circ, 43.9^\circ, 53.5^\circ$ can be indexed to the (1 0 0), (1 0 1) and (0 0 4) planes of MWCNT as shown in Figure 4 [21].

The XRD results suggest that there were good compatibility and interaction between chitosan, lactide and MWCNT in the composite. The interaction causes the decreasing of crystallinity of chitosan, due to the incorporation of amorphous lactide and MWCNT into it, suggesting a hydrogen bonding between them which leads to their good compatibility [14].

4.5. Mechanical Properties

For the mechanical properties analysis a

dynamical-mechanical instrument was used. The mechanical strength affect the ability of the scaffold to be used in tissue engineering. Table 3 exhibits the mechanical properties for the Ch/DL PLG/MWCNT composites. The composite with 20% of MWCNT exhibited the biggest module indicating that it is a more resistant material than other composites.

As MCWNT increases, the elastic module varies from 1.28×10^5 Pa to 2.08×10^5 Pa, corresponding to 10% and 20% content of MWCNT in the composite. The 15% composite displayed a considerable increase in the elastic module when compared to the 10% composite. These results exhibited improved mechanical properties for composite using MWCNT for the use in tissue engineering. It was expected the existence of weak hydrogen bonding between the lactide and chitosan [15], but the improvement in the mechanical properties of the chitosan was observed as the MWCNT content was increased in the composite. As it was suggested in previous research [14], this hydrogen bonding can be between the amino groups of chitosan and carboxiles groups of DL PLG, or between hidroxiles in the chitosan and carboxiles of DL PLG in the blend.

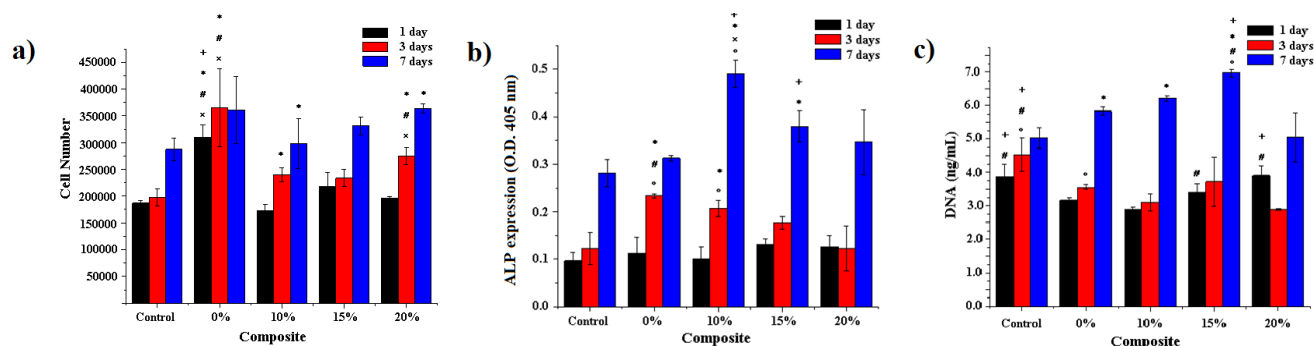


Figure 6. a) Cell number, b) ALP expression graph for the different composites seeded with osteoblasts and c) DNA content of the samples. (+: significant difference compared to 0% composite, *: significant difference compared to control, #: significant difference compared to 10% composite, x: significant difference to 15% composite, and o: significant difference to 20% composite ($p < 0.05$). For the culture, it was used 3 scaffolds of each sample (1 cm^2) for the different biological tests

4.6. Biocompatibility Results

The cell proliferation and viability of the cells was measured using MTT (3-[4,5-dimethylthiazol-2-yl]-2,5-diphenyltetrazolium bromide) assay. This study was used to quantitatively assess the number of viable cells attached and grown on the tested scaffolds [22]. A bar graph for behavior of the cell number of osteoblasts seeded on the different scaffolds is shown in Figure 6a.

According with the results, the Ch/DLPLG/MWCNT composites do not show significantly higher number of cells from day 1 to day 7. After 7 days, cell number increase significantly in Ch/DLPLG/MWCNT 20% composite related with control. Also, Ch/DLPLG/MWCNT 20% composite increase cell number related with control at days 3 and 7. This is similar for composite with 10% of MWCNT at days 3 and 7. DNA content measured in the scaffolds (Figure 6c) is in agreement with cell proliferation results. These results suggest that the MWCNT allows increase or maintain viability in the different combinations. The viability showed by Ch/DLPLG/MWCNT 20% could be due to the percentage of pores in the range of 100-150 μm . These pore sizes have been identified with increased proliferation [15].

The bar graph in Figure 6b illustrates the results of the ALP expression of the osteoblasts in the composites. The ALP expression furthermore shows that Ch/DLPLG/MWCNT increased ALP activity from 3 to 7 days. ALP activity in the composites was significantly higher in almost all composites related with control, except for composite with 20% of MWCNT content at day 3 and 7. The behavior of ALP activity for the osteoblast on the samples is typical during the early stages of differentiation, as the increase in activity during the first 7 days, which coincides with the initiation of the mineralization process [15]. Figure 7a shows the presence of a large amount of globular mineral deposits attached to the scaffolds that was also confirmed by EDS analysis (Figure 7b). It was possible to observe the cells covering the surfaces of the composites at 1 and 3 days.

5. Conclusions

Biodegradable Chitosan/DLPLG/MWCNT composite

have been successfully prepared by using a thermally induced phase separation method. A porous morphology that could be appropriated for vascularization process of osteoblast was found. The obtained results from IR, X-ray diffraction, TGA and DMA suggest a chemical interaction between the polymers; and it is believed that an interaction occurred between the amino group (mainly in chitosan) and carboxyl groups in DL PLG or hydroxyl (mainly in chitosan) and carboxyl groups in the blends. Also, *In vitro* cell culture of Wistar rat's osteoblasts were used to evaluate the phenotype expression of cells in the scaffolds, characterizing the viability and alkaline phosphatase (ALP) activity. Moreover, it was confirmed the mineralization of the cells by IR spectra and EDS analysis. Our results thus show that Ch/DL PLG/MWCNT scaffolds are suitable for biological applications.

ACKNOWLEDGEMENTS

The authors acknowledge the financial support of the Mexican Public Education Secretary and the Mexican National Council for Science and Technology (CONACyT) through project SEP-CONACyT CB 2012-01-180909. Also, the authors appreciate the support of Mr. Armando Cardona Torres during the edition of this document.

REFERENCES

- Jiang T, Nukavarapu SP, Deng M, Jabbarzadeh E, Kofron MD, Doty SB, et al. Chitosan-poly(lactide-co-glycolide) microsphere-based scaffolds for bone tissue engineering: in vitro degradation and in vivo bone regeneration studies. *Acta biomaterialia* 2010;6:3457-70.
- Armentano I, Dottori, M., Fortunati, E., Mattioli, S., Kenny, J. Biodegradable polymer matrix nanocomposites for tissue engineering: a review. 2010;95:2126-46.
- Martel-Estrada SA, Martínez-Pérez CA, Chacón-Nava JG, García-Casillas PE, Olivas-Armendáriz I. In vitro bioactivity of chitosan/poly (d,l-lactide-co-glycolide) composites. *Materials Letters* 2011;65:137-41.

- [4] Liu C, Xia, Z., Czernuszka, J. Design and development of three-dimensional scaffolds for tissue engineering. *Chemical Engineering Research and Design* 2007;1051-64.
- [5] Vukomanovic M, Zavasnik-Bergant T, Bracko I, Skapin SD, Ignjatovic N, Radmilovic V, et al. Poly(D,L-lactide-co-glycolide)/hydroxyapatite core-shell nanospheres. Part 3: properties of hydroxyapatite nano-rods and investigation of a distribution of the drug within the composite. *Colloids and surfaces B, Biointerfaces* 2011;87:226-35.
- [6] Martel-Estrada SA, Olivas-Armendáriz, I., Martínez-Pérez, C.A., Hernández, T., Acosta-Gómez, E.I., Chacón-Nava, J.G., Jiménez-Vega, F., García-Casillas, P.E. Chitosan/poly (DL,lactide-co-glycolide) scaffolds for tissue engineering. *Journal of Materials Science: Materials in Medicine* 2012; 23:2893–901.
- [7] Abdull Rasad MSB, Halim AS, Hashim K, Rashid AHA, Yusof N, Shamsuddin S. In vitro evaluation of novel chitosan derivatives sheet and paste cytocompatibility on human dermal fibroblasts. *Carbohydrate Polymers* 2010;79: 1094-100.
- [8] Ming Yang J, Chih Chiu H. Preparation and characterization of polyvinyl alcohol/chitosan blended membrane for alkaline direct methanol fuel cells. *Journal of Membrane Science* 2012;419-420:65-71.
- [9] Huang Y, Onyeri S, Siewe M, Moshfeghian A, Madihally SV. In vitro characterization of chitosan-gelatin scaffolds for tissue engineering. *Biomaterials* 2005;26:7616-27.
- [10] Chen H-H, Anbarasan R, Kuo L-S, Chen P-H. A novel report on Eosin Y functionalized MWCNT as an initiator for ring opening polymerization of ϵ -caprolactone. *Materials Chemistry and Physics* 2011;126:584-90.
- [11] Theodore M, Hosur M, Thomas J, Jeelani S. Influence of functionalization on properties of MWCNT–epoxy nanocomposites. *Materials Science and Engineering: A* 2011; 528:1192-200.
- [12] Saini P, Choudhary V, Singh BP, Mathur RB, Dhawan SK. Polyaniline–MWCNT nanocomposites for microwave absorption and EMI shielding. *Materials Chemistry and Physics* 2009;113:919-26.
- [13] Gholami F, Zein SHS, Gerhardt L-C, Low KL, Tan SH, McPhail DS, et al. Cytocompatibility, bioactivity and mechanical strength of calcium phosphate cement reinforced with multi-walled carbon nanotubes and bovine serum albumin. *Ceramics International* 2013;39:4975-83.
- [14] Martel-Estrada SA, Martínez-Pérez CA, Chacón-Nava JG, García-Casillas PE, Olivas-Armendariz I. Synthesis and thermo-physical properties of chitosan/poly(dl-lactide-co-glycolide) composites prepared by thermally induced phase separation. *Carbohydrate Polymers* 2010;81:775-83.
- [15] Martel-Estrada SA, Olivas-Armendariz I, Martínez-Pérez CA, Hernández T, Acosta-Gomez EI, Chacon-Nava JG, et al. Chitosan/poly(DL,lactide-co-glycolide) scaffolds for tissue engineering. *Journal of materials science Materials in medicine* 2012;23:2893-901.
- [16] Olivas-Armendariz I, Martel-Estrada SA, Mendoza-Duarte ME, Jiménez-Vega F, García-Casillas P, Martínez-Pérez CA. Biodegradable Chitosan/Multiwalled Carbon Nanotube Composite for Bone Tissue Engineering. *Journal of Biomaterials and Nanobiotechnology* 2013;04:204-11.
- [17] Martel-Estrada SA, Santos-Rodríguez E, Olivas-Armendáriz I, Cruz-Zaragoza E, Martínez-Pérez CA. The effect of radiation on the thermal properties of chitosan/mimosa tenuiflora and chitosan/mimosa tenuiflora/multiwalled carbon nanotubes (MWCNT) composites for bone tissue engineering. 2014:55-64.
- [18] Lewandowska K. Miscibility and thermal stability of poly(vinyl alcohol)/chitosan mixtures. *Thermochimica Acta* 2009;493:42-8.
- [19] Pasanphan W, Rattanawongwiboon, T., Choofong, S., Güven, O., Katti, K. Irradiated chitosan nanoparticle as a water-based antioxidant and reducing agent for a green synthesis of gold nanoplateforms. *Radiation Physics and Chemistry* 2015;106: 360-70.
- [20] Souza B, Cerqueira, M., Martins, J., Casariego, A., Teixeira, J., Vicente, A. Influence of electric fields on the structure of chitosan edible coatings. *Food Hydrocolloids* 2010;24:330-5.
- [21] Saleh TA, Agarwal S, Gupta VK. Synthesis of MWCNT/MnO₂ and their application for simultaneous oxidation of arsenite and sorption of arsenate. *Applied Catalysis B: Environmental* 2011.
- [22] Li H. Preparation and Characterization of Homogeneous Hydroxyapatite/Chitosan Composite Scaffolds via In-Situ Hydration. *Journal of Biomaterials and Nanobiotechnology* 2010;01:42-9.